

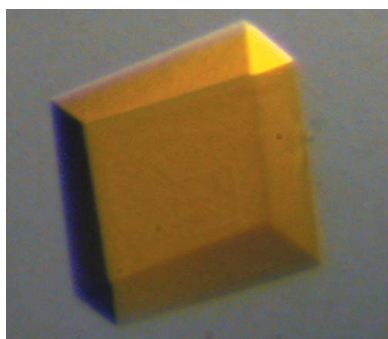
Takashi Umeda,^{a,†} Junichi
Katsuki,^{a,†} Yuji Ashikawa,^{a,b}
Yusuke Usami,^a Kengo Inoue,^a
Haruko Noguchi,^a Zui Fujimoto,^c
Hisakazu Yamane^a and Hideaki
Nojiri^{a,d,*}

^aBiotechnology Research Center, The University of Tokyo, 1-1-1 Yayoi, Bunkyo-ku, Tokyo 113-8657, Japan, ^bMolecular Signaling Research Team, Structural Physiology Research Group, RIKEN Harima Institute SPring-8 Center, 1-1-1 Kouto, Sayo, Hyogo 679-5148, Japan, ^cProtein Research Unit, National Institute of Agrobiological Sciences, 2-1-2 Kannondai, Tsukuba, Ibaraki 305-8602, Japan, and ^dProfessional Programme for Agricultural Bioinformatics, The University of Tokyo, 1-1-1 Yayoi, Bunkyo-ku, Tokyo 113-8657, Japan

† These authors contributed equally to this paper.

Correspondence e-mail:
anojiri@mail.ecc.u-tokyo.ac.jp

Received 4 January 2010
Accepted 20 April 2010



© 2010 International Union of Crystallography
All rights reserved

Crystallization and preliminary X-ray diffraction studies of a ferredoxin reductase component of carbazole 1,9a-dioxygenase from *Novosphingobium* sp. KA1

Carbazole 1,9a-dioxygenase (CARDO) is the initial enzyme of the carbazole-degradation pathway. The CARDO of *Novosphingobium* sp. KA1 consists of a terminal oxygenase, a putidaredoxin-type ferredoxin and a ferredoxin-NADH oxidoreductase (Red) and is classified as a class IIA Rieske oxygenase. Red from KA1 was crystallized at 278 K by the hanging-drop vapour-diffusion method using PEG 4000. The crystal diffracted to 1.58 Å resolution and belonged to space group $P3_2$, with unit-cell parameters $a = b = 92.2$, $c = 78.6$ Å, $\alpha = \gamma = 90$, $\beta = 120^\circ$. Preliminary analysis of the X-ray diffraction data revealed that the asymmetric unit contained two Red monomers. The crystal appeared to be a merohedral twin, with a twin fraction of 0.32 and twin law $(-h, -k, l)$.

1. Introduction

Carbazole 1,9a-dioxygenase (CARDO), a member of the Rieske nonhaem iron oxygenases (ROs), catalyses the regioselective and stereoselective dihydroxylation of carbazole and acts as a primary catalyst in the degradation of carbazole by various bacteria. CARDO consists of three components: a terminal oxygenase (Oxy; encoded by the *carAa* gene), a ferredoxin (Fd; encoded by the *carAc* or *fdx* gene) and a ferredoxin reductase (Red; encoded by the *carAd* or *fdr* gene). *Novosphingobium* sp. KA1 possesses the carbazole-degradative plasmid pCAR3 (Shintani *et al.*, 2007), which contains two CARDO genes (*carAa1CarAc1*, *carAa1Ac12*, *fdx1* and *fdr1/fdr2*).

ROs can be divided into five subgroups (IA, IB, IIA, IIB and III) based on their number of constituents and the nature of their redox centre (Batie *et al.*, 1991). There are three types of RO reductases: class IA reductases contain FMN and a plant-type [2Fe–2S] cluster; class IB and III reductases contain FAD and a plant-type [2Fe–2S] cluster; and class IIA and IIB reductases contain FAD as their cofactor. Class IIA and IIB reductases are grouped into the bacterial oxygenase-coupled NADH-ferredoxin reductases (ONFRs). ONFRs are members of the glutathione reductase-type ferredoxin-NADP⁺ oxidoreductases (GR-type FNRs). Aliverti *et al.* (2008) have written an excellent review on GR-type FNRs.

The CARDOs of KA1 are classified as class IIA ROs. Other well studied CARDOs from *Pseudomonas resinovorans* CA10, *Janthinobacterium* sp. J3 and *Nocardioides aromaticivorans* IC177 have been grouped into classes III, III and IIB, respectively. Therefore, the CARDO system has two different types of Reds, although high primary sequence similarity exists in the Oxy (>45% identity and >70% similarity) between the three classes, as well as a similarity in the reactions catalysed.

Recently, we have reported several crystal structures of the components of CARDOs: Fd_{III} from *P. resinovorans* CA10 (Nam *et al.*, 2005), Oxy_{III} from *Janthinobacterium* sp. J3 (Nojiri *et al.*, 2005), their electron-transfer complex (Ashikawa *et al.*, 2006) and Oxy_{IIB} and Fd_{IIB} from *N. aromaticivorans* (Inoue *et al.*, 2009). We have also crystallized Red_{III} from *Janthinobacterium* sp. J3 (Ashikawa *et al.*, 2007) and Fd_{IIA} from *Novosphingobium* sp. KA1 (Umeda *et al.*, 2008). To date, several structures of RO reductases and related reductases have been determined: phthalate dioxygenase reductase (class IA; Correll *et al.*, 1992), benzoate dioxygenase reductase (class IB; Karlsson *et al.*, 2002), biphenyl dioxygenase reductase (class IIB;

36.5% sequence identity to Red_{IIA}; Senda *et al.*, 2000), toluene dioxygenase reductase (class IIB; 30.2% sequence identity to Red_{IIA}; Friemann *et al.*, 2009) and putidaredoxin reductase (41.3% sequence identity to Red_{IIA}; Sevrioukova *et al.*, 2004). However, no structure of a class IIA RO reductase has been reported. In this paper, we describe the crystallization and preliminary X-ray diffraction study of Red_{IIA} (encoded by *fdrII*, 420 amino-acid residues, 44.4 kDa molecular mass). The three-dimensional structure of class IIA Red will provide additional insight into the mechanisms of electron transfer and recognition of a suitable redox partner between RO components.

2. Experimental methods

2.1. Cloning

Total DNA of *Novosphingobium* sp. KA1 was used as a template for PCR. The following oligonucleotides were used as primers: 5'-AAA AAA GGT ACC ATA AGG AGG TGT TCA TAT GCA CCA CCA CCA CCA CCA CGC TGA TAT CGT TAT TGT C-3' and 5'-AAA AAA GAA TTC TCA AAC AGC GGC TCC GCC GTT-3'; the *NdeI* (forward primer) and *EcoRI* (reverse primer) restriction sites are shown in bold and a His₆-tag sequence is shown in italics. The His₆ tag was inserted between the starting methionine residue and the following alanine residue. The PCR-amplified and doubly digested gene products were ligated into the pET26b(+) expression vector and named pEKA240.

2.2. Expression and purification

The expression strain *Escherichia coli* BL21 (DE3) was transformed with pEKA240. Overnight cultured cells grown in 5 ml lysogeny (L) medium (10 g tryptone peptone, 5 g yeast extract and 10 g NaCl per litre; Sambrook & Russell, 2001) at 310 K were used to inoculate 1.5 l SB medium (12 g tryptone, 24 g yeast extract, 3.8 g KH₂PO₄ and 12.5 g K₂HPO₄ per litre) containing kanamycin (50 µg ml⁻¹). Cultivation was carried out at 298 K and 120 rev min⁻¹ until the optical density at 600 nm reached 0.4–0.5. Subsequently, isopropyl β-D-1-thiogalactopyranoside was added to a final concentration of 0.2 mM. Cells were grown for 12 h and then harvested by centrifugation at 5000g for 10 min. The cell pellet was washed twice with TG buffer (20 mM Tris–HCl pH 7.5 and 10% glycerol). The cells

were then suspended in buffer A (TG buffer containing 0.5 M NaCl) and sonicated for 10 min at 277 K. The crude extract was clarified by ultracentrifugation (25 000g for 60 min at 277 K); the pellet was discarded and the supernatant was stored on ice. The supernatant was loaded onto a HiTrap Chelating HP column (GE Healthcare, UK) pre-equilibrated with buffer A on an ÄKTA FPLC instrument (GE Healthcare, UK). Red_{IIA} was eluted with 0–300 mM imidazole in buffer A. The eluted fraction containing Red_{IIA} was concentrated and buffer-exchanged with GFC buffer (20 mM Tris–HCl pH 7.5, 0.2 M NaCl and 10% glycerol) by ultrafiltration using a Centriprep YM-10 (Millipore, USA) device and then subjected to gel-filtration chromatography using a Superdex 200 prep-grade column (GE Healthcare, UK). Prior to loading the protein sample, the gel-filtration column was equilibrated with GFC buffer. The protein was eluted from the column and collected as 2 ml fractions. Fractions were analysed by SDS–PAGE and Red_{IIA} was pooled, concentrated and buffer-exchanged with crystallization buffer (5 mM Tris–HCl) as described above. The protein concentration was estimated using a protein-assay kit (Bio-Rad, USA) according to the method of Bradford (1976) using BSA as a standard.

2.3. Crystallization

Protein solutions containing 5, 10, 20 and 30 mg ml⁻¹ Red_{IIA} were used to set up initial crystallization screening experiments at 278 K. The hanging-drop vapour-diffusion method was used, with a drop size of 6 µl (3 µl protein solution and 3 µl reservoir solution) and 600 µl reservoir solution. Screening was carried out using Crystal Screens I, II and Cryo, Index Screen and Grid Screen Ammonium Sulfate (Hampton Research, USA). Crystals appeared within a week in several conditions that contained polyethylene glycol as precipitant. After optimization of Crystal Screen condition No. 40, the reservoir solution was composed of 0.0475 M trisodium citrate dihydrate pH 5.6, 9.5%(v/v) 2-propanol, 9.5%(w/v) PEG 4000, 2.5%(v/v) glycerol and 0.2 M caesium chloride.

2.4. Diffraction data collection and processing

A single crystal of Red_{IIA} was soaked in reservoir solution containing 15% glycerol and flash-cooled in a nitrogen stream at 100 K. Diffraction data collection was carried out on beamline NW12A of Photon Factory, Tsukuba, Japan, which is equipped with an ADSC Quantum 210r CCD detector. The data set was collected from a single crystal at a wavelength of 1.000 Å in 0.5° oscillation steps over a range of 240° with 30 s exposure per frame. The data were indexed, integrated and merged to a resolution of 1.58 Å using the *HKL-2000* program suite (Otwinowski & Minor, 1997). The criterion for determination of the resolution range used was the resolution at which R_{merge} remained less than 0.45.

3. Results and discussion

3.1. Purification and crystallization of Red_{IIA}

10 mg of Red_{IIA} was purified from 1.5 l of culture. During the gel-filtration experiments, the eluted Red_{IIA} corresponded to a molecular mass of approximately 39.8 kDa (data not shown). Similar to the reductase component of toluene dioxygenase from *P. putida* F1 (Subramanian *et al.*, 1981), Red_{IIA} is a monomer in solution, although BphA4, a ferredoxin reductase component of biphenyl dioxygenase from *Acidovorax* sp. KKS102, eluted as a dimer (Senda *et al.*, 2000). SDS–PAGE analysis estimated the purified Red_{IIA} product to be >95% pure (Fig. 1, lane 4). A well diffracting rhombic shaped crystal

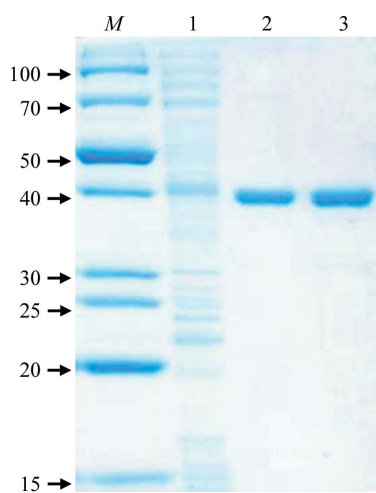


Figure 1
12% SDS–PAGE gel run to assess the effectiveness of the purification procedure. Lane M, marker proteins (kDa); lane 1, cell lysate; lane 2, pooled Red_{IIA} fractions after affinity chromatography; lane 3, pooled Red_{IIA} fractions after gel-filtration chromatography.

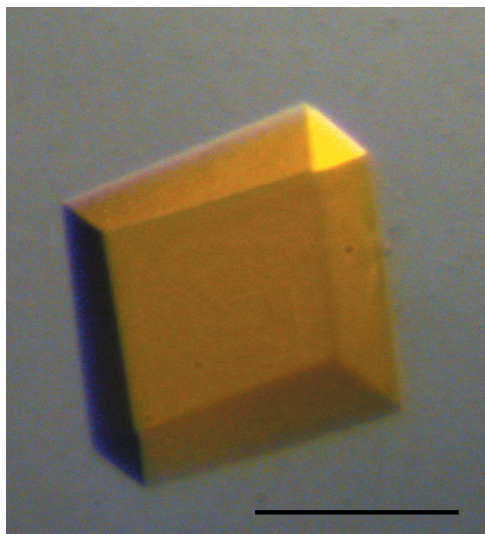


Figure 2
A Red_{IIA} crystal. The scale bar indicates 0.16 mm.

Table 1

Crystal parameters and data-collection statistics.

Values in parentheses are for the highest resolution shell.

Wavelength (Å)	1.000
Space group	$P3_2$
Unit-cell parameters (Å, °)	$a = b = 92.2, c = 78.6,$ $\alpha = \beta = 90, \gamma = 120$
Resolution range (Å)	30.0–1.58
Total No. of reflections	780087
No. of unique reflections	102170 (10235)
Completeness (%)	100 (100)
Average $I/\sigma(I)$	54.9 (4.7)
$R_{\text{merge}}^{\dagger}$ (%)	10.4 (42.5)
Multiplicity	7.6 (7.5)

$\dagger R_{\text{merge}} = \frac{\sum_{hkl} \sum_i |I_i(hkl) - \langle I(hkl) \rangle|}{\sum_{hkl} \sum_i I_i(hkl)}$, where $I_i(hkl)$ is the i th observation of reflection hkl and $\langle I(hkl) \rangle$ is the weighted average intensity for all observations of reflection hkl .

of Red_{IIA} (Fig. 2) was obtained after 1 d of incubation at a protein concentration of 20 mg ml⁻¹ at 278 K and grew to largest dimensions of 0.3 × 0.3 × 0.1 mm; typical dimensions were 0.2 × 0.2 × 0.05 mm.

3.2. Data collection and analysis of the diffraction data

The crystal belonged to space group $P3_2$, with unit-cell parameters $a = b = 92.2, c = 78.6$ Å, $\alpha = \gamma = 90, \beta = 120^\circ$, and presumably contained two monomers in the asymmetric unit. This resulted in a solvent content of 45% and a favourable V_M (Matthews, 1968) of 2.04 Å³ Da⁻¹. Solution of the structure was attempted by molecular replacement using the crystal structure of putidaredoxin reductase (PDB code 1q1r; Sevrionkova *et al.*, 2004) as a model. As expected, molecular replacement found two solutions, corresponding to a noncrystallographic dimer of Red_{IIA}, in the asymmetric unit. The R factor and R_{free} fell to approximately 30% after initial rounds of crystallographic refinement. However, further refinement failed to lead to an R_{free} factor below 30%, although the electron-density map

showed good coincidence with the model structure. Re-examination of the diffraction data indicated that the crystal appeared to be merohedrally twinned. The data were analysed and detwinned using the program *DETWIN* (Collaborative Computational Project, Number 4, 1994), which revealed a twin fraction of 0.32 with a twin law $(-h, -k, l)$. Data-collection statistics are given in Table 1.

A detailed description of the crystal structure, including the structure determination and refinement, of Red_{IIA} will be reported elsewhere.

This work was supported by Grants-in-Aid for Scientific Research (17380052 and 20248010 to HN) from the Ministry of Education, Culture, Sports, Science and Technology of Japan and by the Institute for Bioinformatics Research Development, Japan Science Technology Agency (BIRD-JST). The use of synchrotron radiation was approved by the Photon Factory Advisory Committee and KEK (High-Energy Accelerator Research Organization), Tsukuba (proposals 2004G137, 2006G171, 2007G135 and 2008G681).

References

- Aliverti, A., Pandini, V., Pennati, A., de Rosa, M. & Zanetti, G. (2008). *Arch. Biochem. Biophys.* **474**, 283–291.
- Ashikawa, Y., Fujimoto, Z., Noguchi, H., Habe, H., Omori, T., Yamane, H. & Nojiri, H. (2006). *Structure*, **14**, 1779–1789.
- Ashikawa, Y., Uchimura, H., Fujimoto, Z., Inoue, K., Noguchi, H., Yamane, H. & Nojiri, H. (2007). *Acta Cryst.* **F63**, 499–502.
- Batie, C. J., Ballou, D. P. & Correll, C. C. (1991). *Chemistry and Biochemistry of Flavoenzymes*, edited by F. Muller, Vol. 3, pp. 543–556. Boca Raton: CRC Press.
- Bradford, M. M. (1976). *Anal. Chem.* **72**, 248–254.
- Collaborative Computational Project, Number 4 (1994). *Acta Cryst.* **D50**, 760–763.
- Correll, C. C., Batie, C. J., Ballou, D. P. & Ludwig, M. L. (1992). *Science*, **258**, 1604–1610.
- Friemann, R., Lee, K., Brown, E. N., Gibson, D. T., Eklund, H. & Ramaswamy, S. (2009). *Acta Cryst.* **D65**, 24–33.
- Inoue, K., Ashikawa, Y., Umeda, T., Abo, M., Katsuki, J., Usami, Y., Noguchi, H., Fujimoto, Z., Terada, T., Yamane, H. & Nojiri, H. (2009). *J. Mol. Biol.* **392**, 436–451.
- Karlsson, A., Beharry, Z. M., Eby, D. M., Coulter, E. D., Neidle, E. L., Kurtz, D. M. Jr, Eklund, H. & Ramaswamy, S. (2002). *J. Mol. Biol.* **318**, 261–272.
- Matthews, B. W. (1968). *J. Mol. Biol.* **33**, 491–497.
- Nam, J.-W., Noguchi, H., Fujimoto, Z., Mizuno, H., Ashikawa, Y., Abo, M., Fushinobu, S., Kobashi, N., Wakagi, T., Iwata, K., Yoshida, T., Habe, H., Yamane, H., Omori, T. & Nojiri, H. (2005). *Proteins*, **58**, 779–789.
- Nojiri, H., Ashikawa, Y., Noguchi, H., Nam, J.-W., Urata, M., Fujimoto, Z., Uchimura, H., Terada, T., Nakamura, S., Shimizu, K., Yoshida, T., Habe, H. & Omori, T. (2005). *J. Mol. Biol.* **351**, 355–370.
- Otwinowski, Z. & Minor, W. (1997). *Methods Enzymol.* **276**, 307–326.
- Sambrook, J. & Russell, D. W. (2001). *Molecular Cloning: A Laboratory Manual*, 3rd ed. New York: Cold Spring Harbor Laboratory Press.
- Senda, T., Yamada, T., Sakurai, N., Kubota, M., Nishizaki, T., Masai, E., Fukuda, M. & Mitsui, Y. (2000). *J. Mol. Biol.* **304**, 397–410.
- Sevrionkova, I. F., Li, H. & Poulos, T. L. (2004). *J. Mol. Biol.* **336**, 889–902.
- Shintani, M., Urata, M., Inoue, K., Eto, K., Habe, H., Omori, T., Yamane, H. & Nojiri, H. (2007). *J. Bacteriol.* **189**, 2007–2020.
- Subramanian, V., Liu, T.-N., Yeh, W.-K., Narro, M. & Gibson, D. T. (1981). *J. Biol. Chem.* **256**, 2723–2730.
- Umeda, T., Katsuki, J., Usami, Y., Inoue, K., Noguchi, H., Fujimoto, Z., Ashikawa, Y., Yamane, H. & Nojiri, H. (2008). *Acta Cryst.* **F64**, 632–635.